



# Initiations of Mesoscale Convective Systems in the Middle Reaches of the Yangtze River Basin : Statistical Characteristics and Environmental Conditions

Ya-Nan Fu<sup>1, 2 + %</sup>, Jian-Hua Sun<sup>1, 2, 3 #</sup>, Shen-Ming Fu<sup>4</sup>, Yuan-Chun Zhang<sup>1</sup>, Zheng Ma<sup>1</sup>

1. Key Laboratory of Cloud-Precipitation Physics and Severe Storms, Institute of Atmospheric Physics, Chinese Academy of Sciences, Beijing, China

2. University of Chinese Academy of Sciences, Beijing, China

3. Collaborative Innovation Center on Forecast and Evaluation of Meteorological Disasters, Nanjing University of Information Science and Technology, Nanjing, China

4. International Center for Climate and Environment Sciences, Institute of Atmospheric Physics, Chinese Academy of Sciences, Beijing, China

03 AUG 2023

SINGAPORE

# Contents

1

Motivation

2

Data & Methodology

3

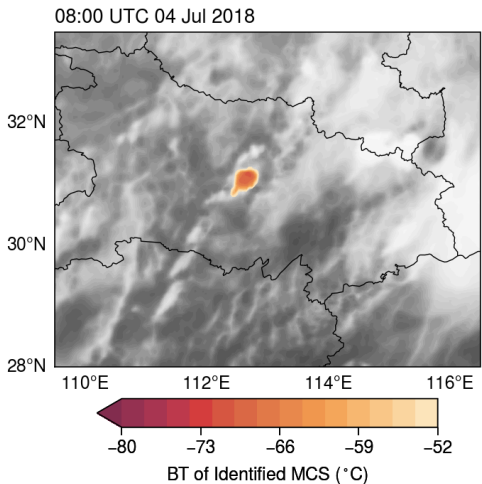
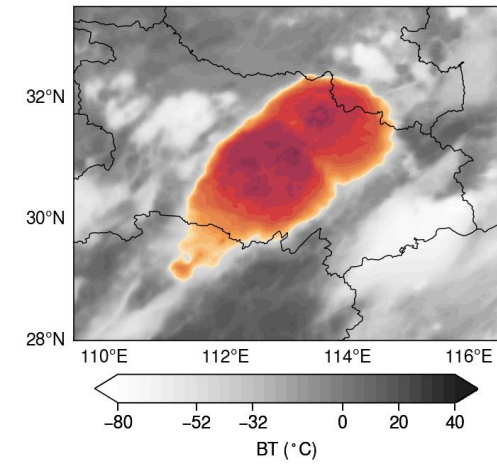
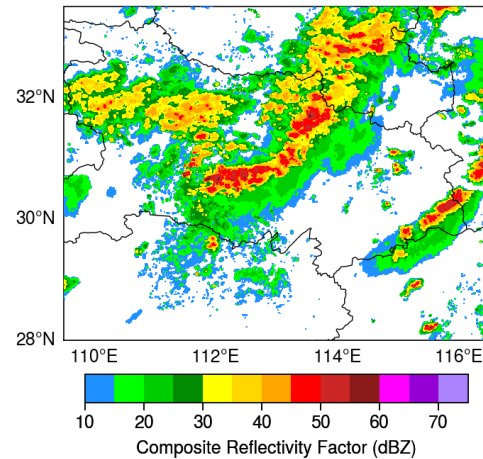
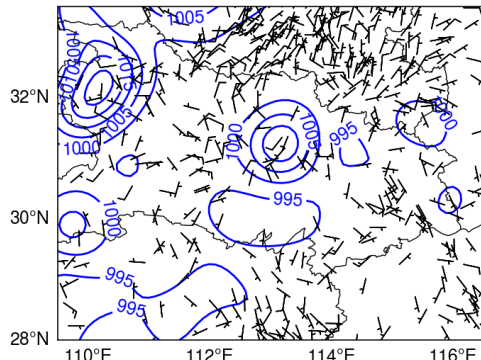
Results

4

Conclusions

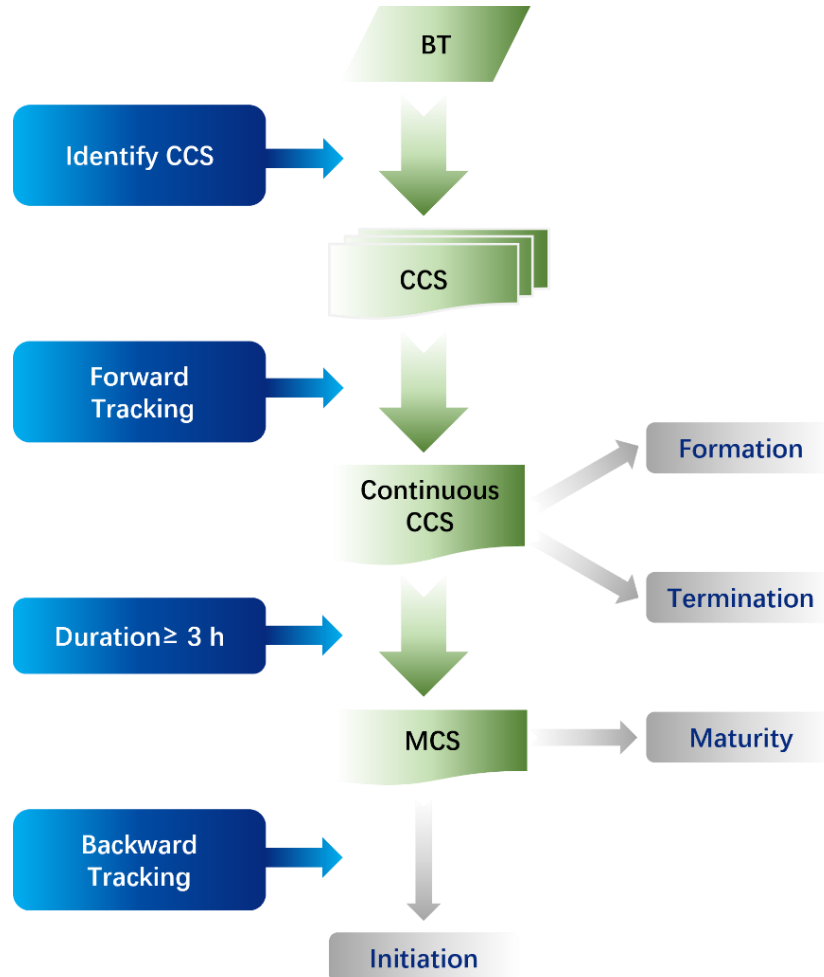
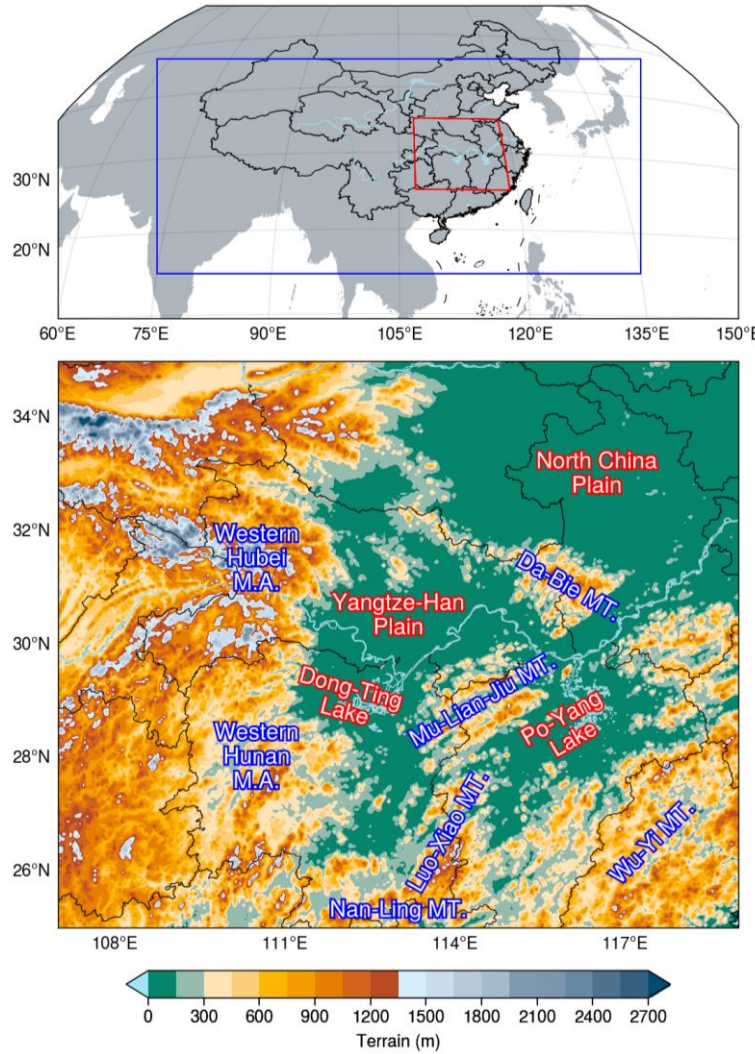
# MOTIVATION

## An MCS case on 4 July 2018



- Severe convective weather phenomena are mainly associated with mesoscale convective systems (MCSs) (Houze, 2004; Zheng et al., 2013), and MCSs exhibit different forms if different techniques of detection and identification are employed.
- On satellite infrared images, MCSs often appear as cold-cloud shields (CCSs) with a certain temporal and spatial scale (Ai et al., 2016; Meng et al., 2021; Yang et al., 2015; Zheng et al., 2008).
- Roberts and Rutledge (2003) found that the precursor signal of convection initiation (CI) can be captured on satellites, suggesting that the entire process of MCS development, from convection initiation to MCS formation, maturation and dissipation, can be tracked in a continuous manner (Ai et al., 2016; Zhang X. et al., 2021).

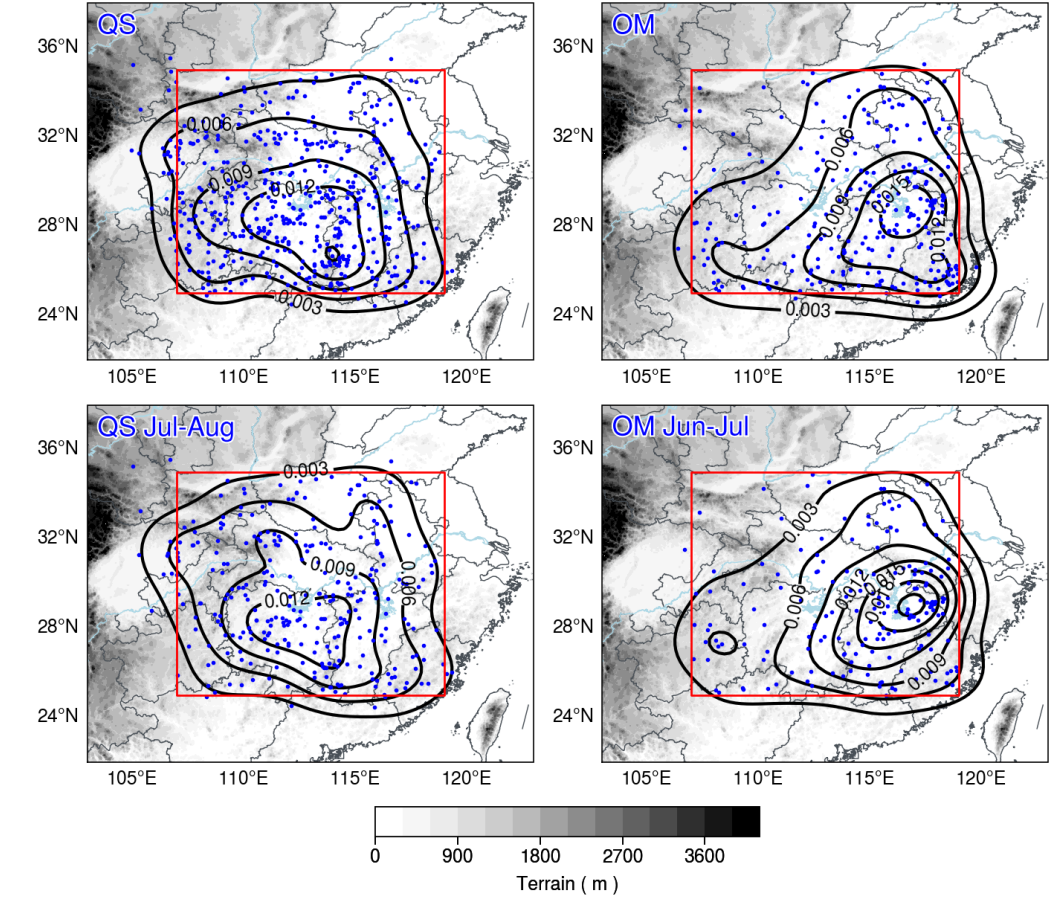
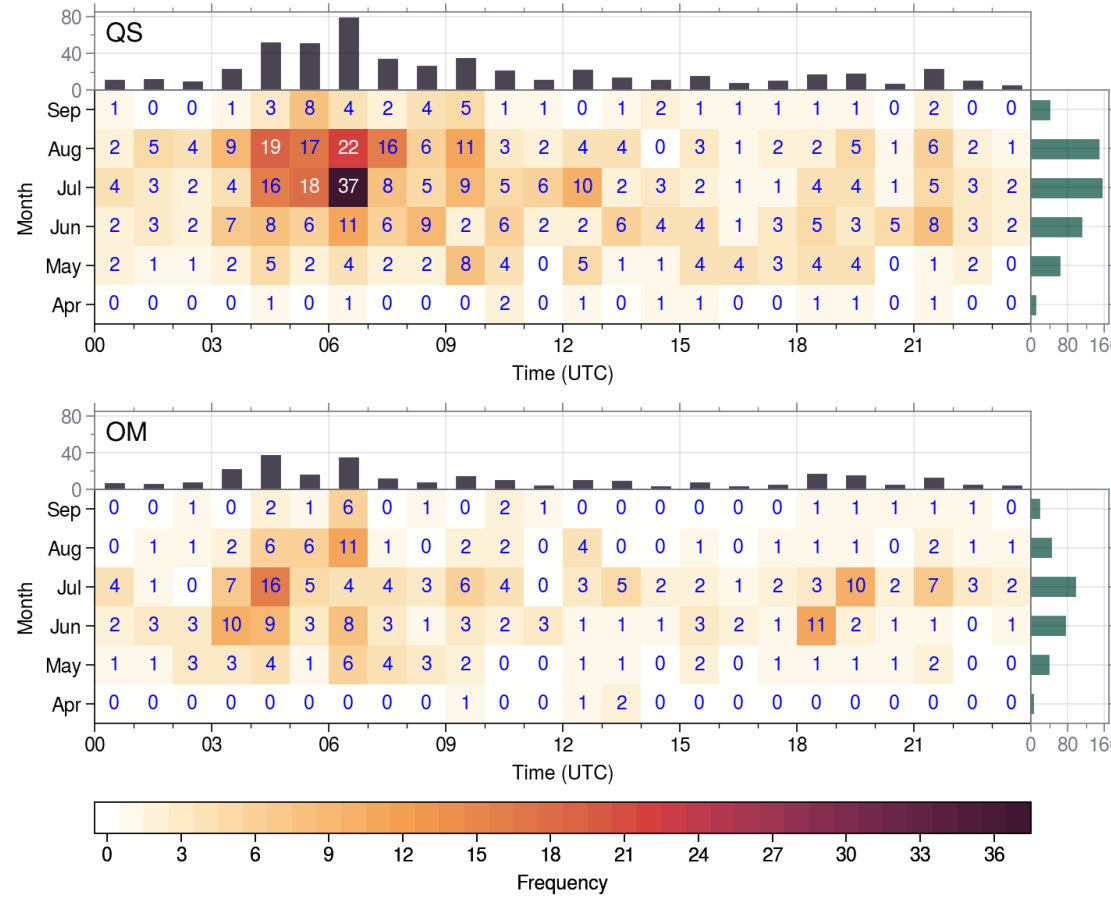
# DATA & METHODOLOGY



<b>Data</b>	FY-4A 10.8 $\mu\text{m}$ BT ERA5
<b>MCS identification</b>	BT $\leq -52^\circ\text{C}$ extent $\geq 5000 \text{ km}^2$ duration $\geq 3 \text{ h}$
<b>MCS tracking</b>	optical flow areal overlap
<b>Classification</b>	k-means silhouette coefficient

# RESULTS

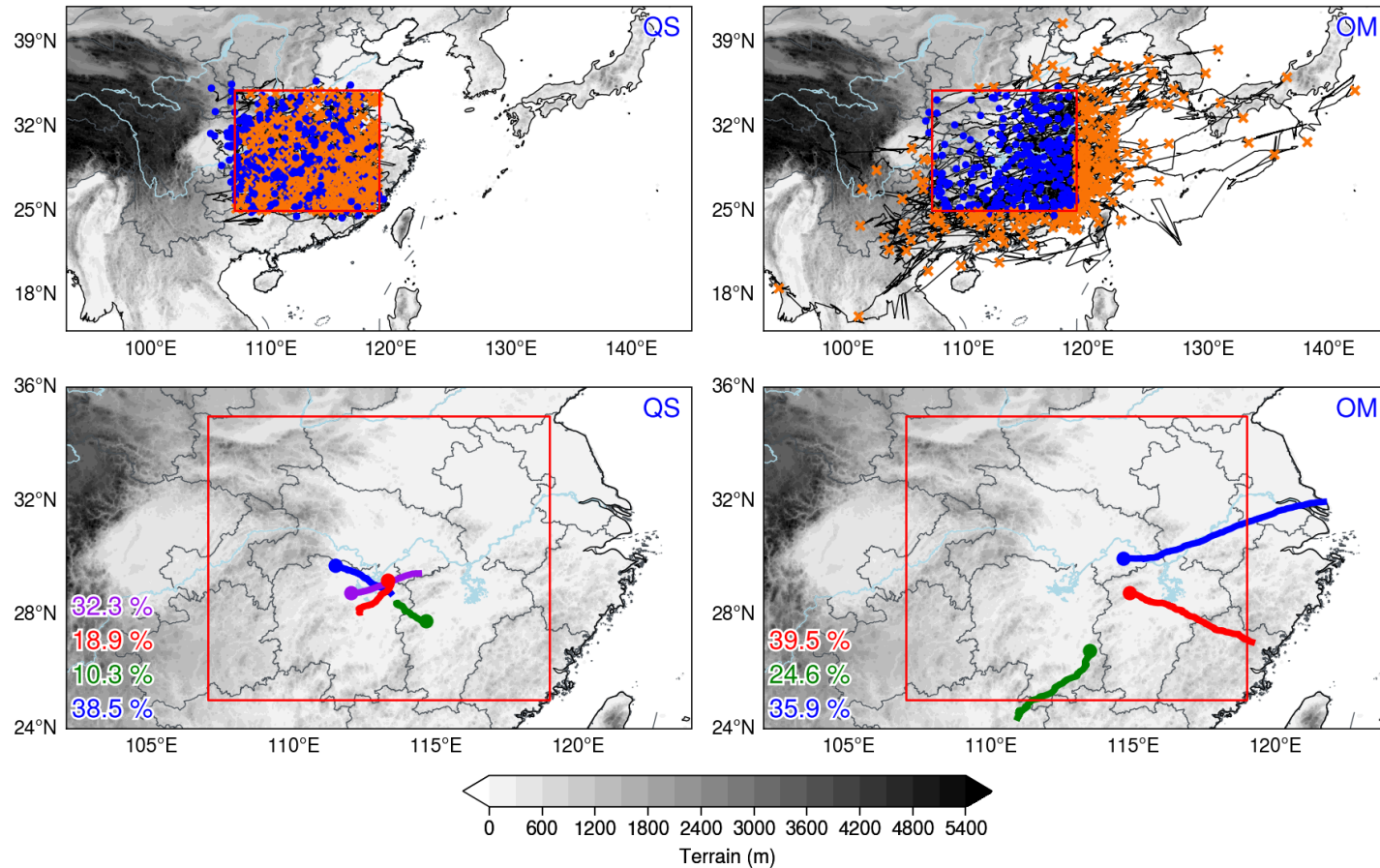
## Temporal-spatial distribution of MCS initiations



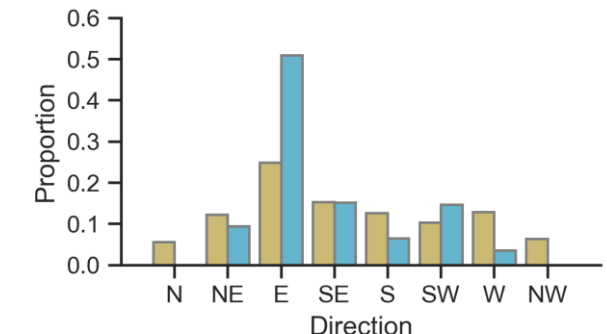
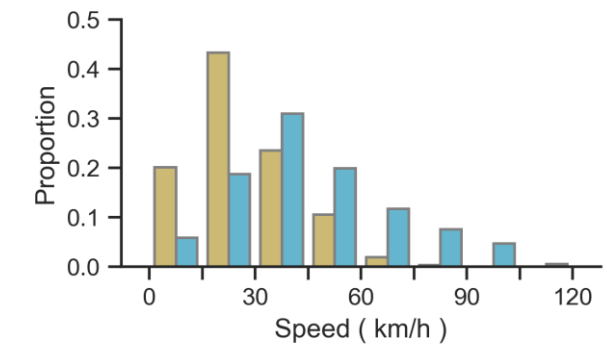
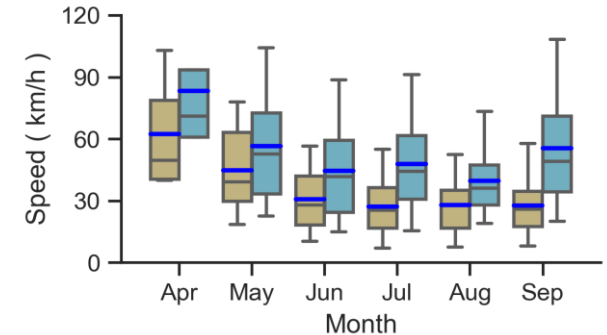
- The QS MCSs primarily occur in July and August and are mainly initiated in the afternoon. The OM MCSs mostly occur in June and July with two initiation peaks at noon and late night, respectively.
- QS MCSs are mainly initiated in mountainous areas and caused by local thermal effects, while OM MCSs are mostly triggered in plain areas, which is related to synoptic circulation forcing.

# RESULTS

## MCS movements

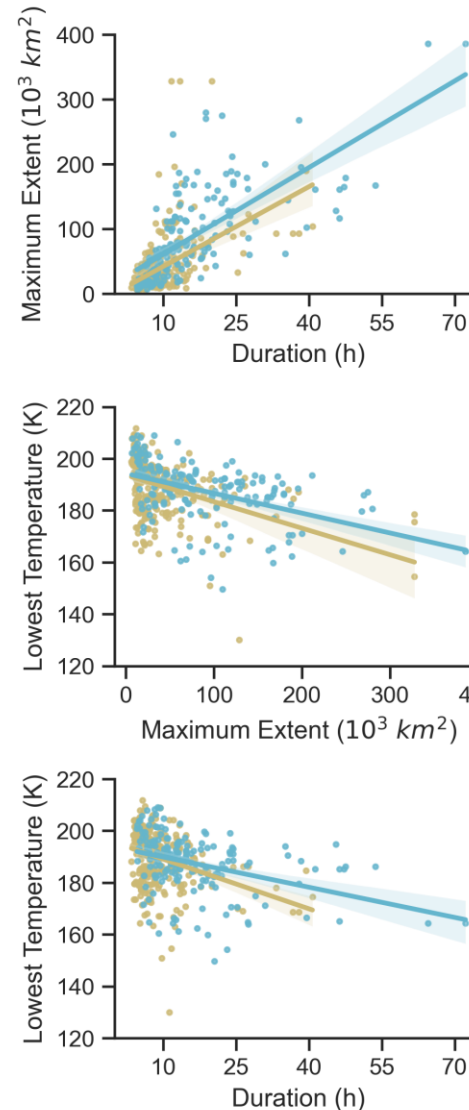
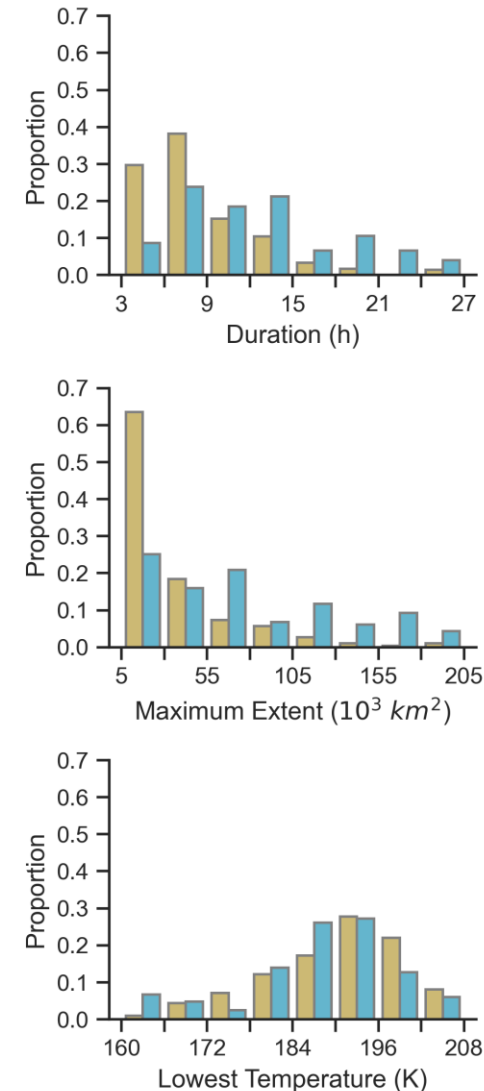
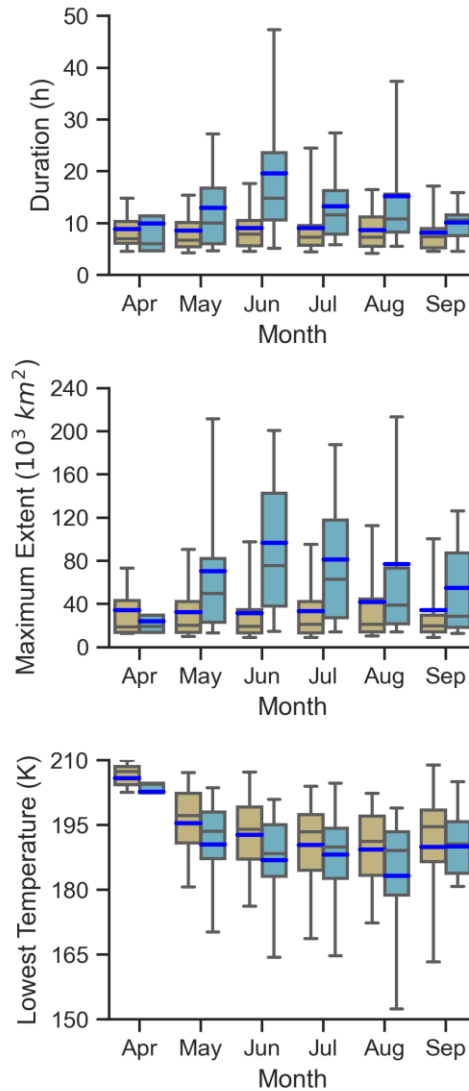


- The trajectories of QS (OM) MCSs are classified into 4 (3) paths using k-means algorithm.
- Convections are initiated in mountainous areas and propagate to the plains.
- The OM MCSs move faster than the QS MCSs and mostly propagate eastward.



# RESULTS

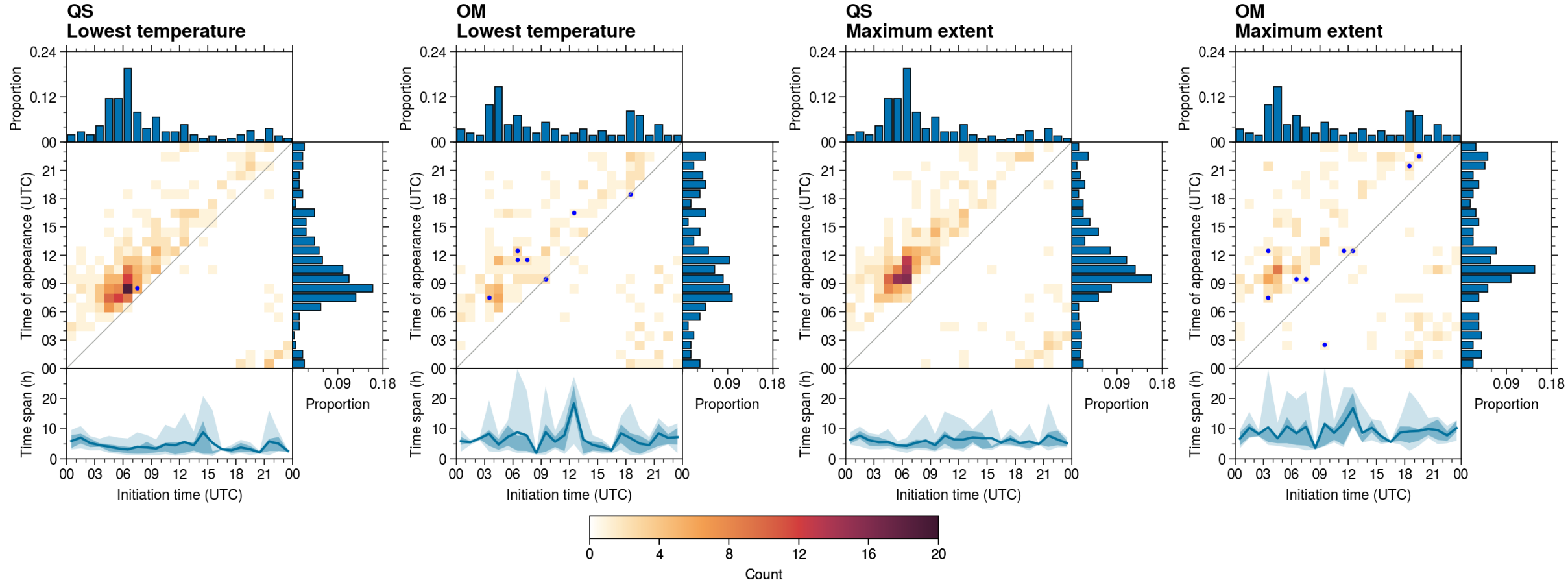
## Duration, maximum extent and lowest temperature



- All three features of QS-MCSs show no obvious differences among different months, but for OM-MCSs, the durations and maximum extents vary notably from month to month.
- In general, the longer the durations of the MCSs are, the larger the maximum extents and the colder the cloud tops.

# RESULTS

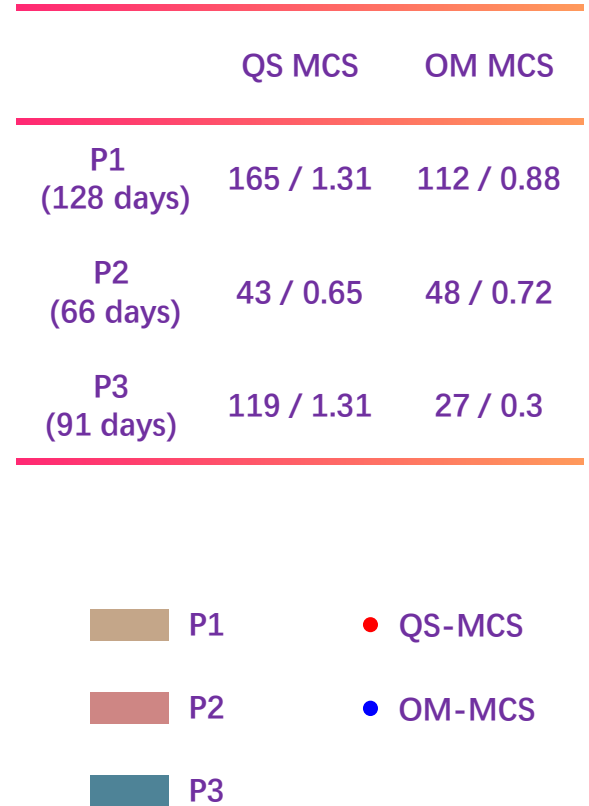
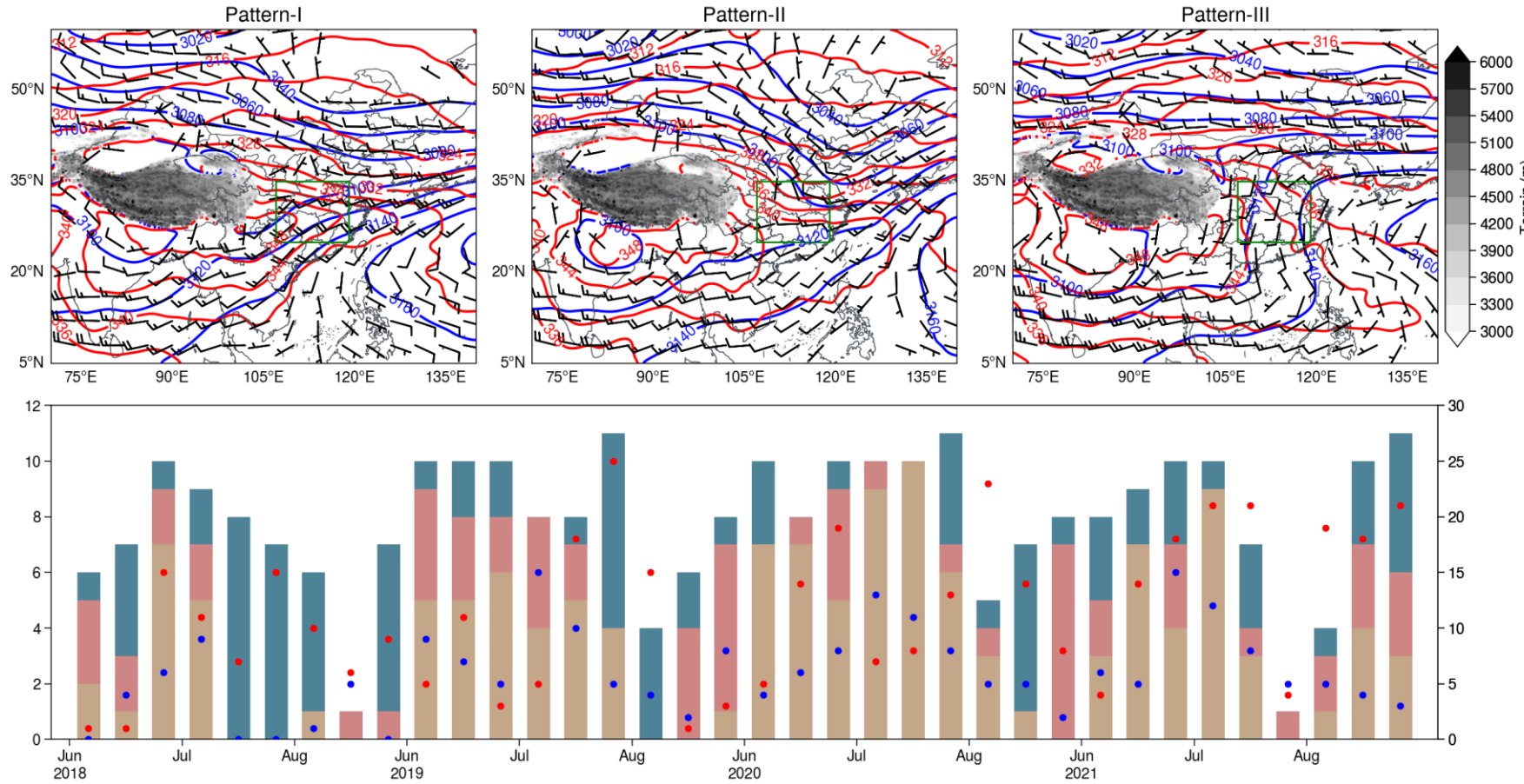
## Development features of MCSs



- The lowest temperatures of QS MCSs mainly appear in the afternoon, while the appearances of the lowest temperatures of OM MCSs are mainly distributed from the afternoon to the evening, without no obvious peaks.
- The lowest temperatures (the maximum extents) of the QS MCSs appear 4.43 h (6.03 h) after initiation, while the lowest temperatures (maximum extents) of the OM MCSs appear 6.8 h (9.21 h) after initiation

# RESULTS

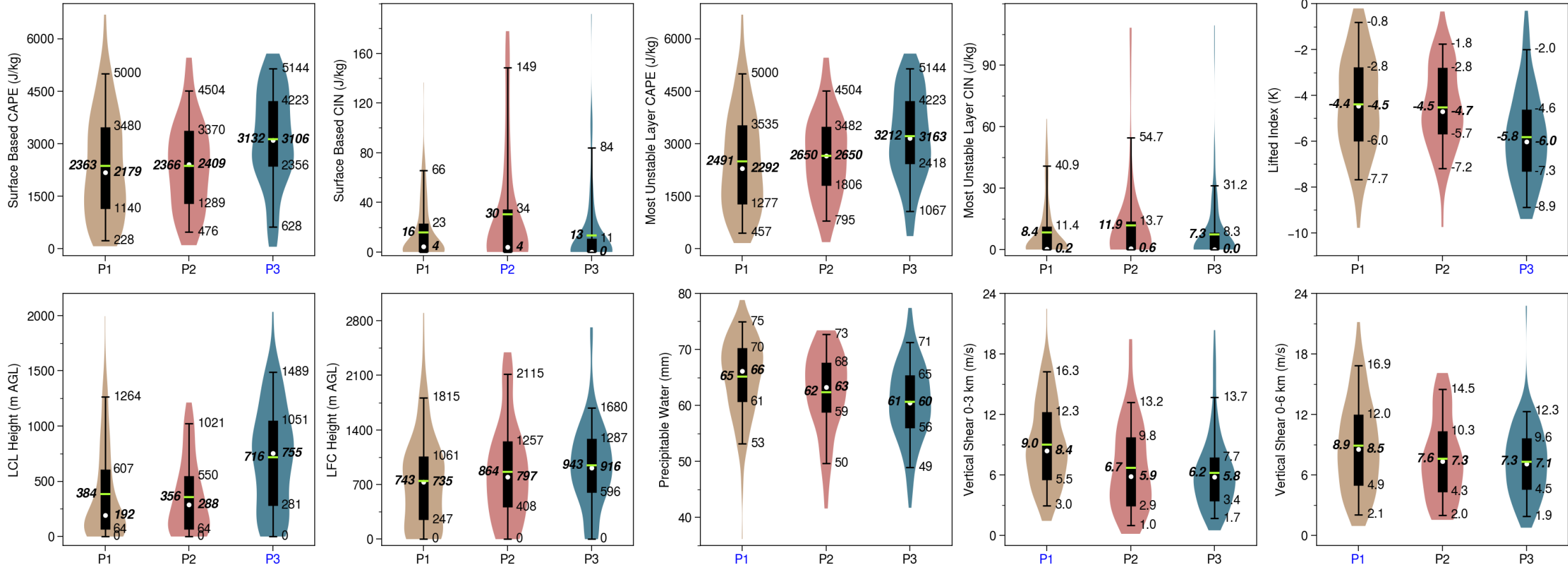
## Circulation patterns



- P1 is the typical circulation of the Mei-yu front. In P2, the middle reaches of the YRB are basically under the control of the northwesterly. In P3, the middle reaches of the YRB are under the control of the weak southerly.
- The occurrence frequency of P1 favors June and July, and that of P2 favors late July and August. The occurrence frequency of OM MCSs peaks in late June or early July, and that of QS MCSs peaks variously in different years.

# RESULTS

## Environmental conditions



- The low-level wind speed in P1 is relatively high, and the MCS initiations in P1 may be accompanied by low-level jets, which is more favorable for OM MCS initiation and propagation.
- The circulation in P2 is dominated by northwesterlies with a relatively stable layer in the low-level troposphere.
- Surface solar heating in P3 establishes a dry-adiabatic layer and further lowers the stability.

## CONCLUSIONS

- During the warm seasons of 2018–2021, 524 QS MCSs and 276 OM MCSs are identified in the middle reaches of the YRB. Among the four kinds of main moving paths (i.e., northeast kind, southeast kind, northwest kind and southwest kind) of QS MCSs, the occurrence frequency in the southeast kind is the highest. The QS MCSs are mostly initiated over mountainous areas and then propagate to the plains. The moving trajectories of OM MCSs are classified into three kinds of paths, namely, the northeast kind, the southeast kind and the southwest kind, among which the southeast kind has the largest amount of OM MCSs.
- The QS MCSs primarily occur in July and August and are mainly initiated in the afternoon (0600–0700 UTC). The OM MCSs mostly occur in June and July with two initiation peaks at noon (0300–0500 UTC) and late night (1800–1900 UTC), respectively, corresponding to the afternoon peak and morning peak of the typical precipitation associated with Mei-yu fronts. QS MCSs are mainly initiated in mountainous areas, while OM MCSs are mostly triggered in plain areas.
- The OM MCSs move faster than the QS MCSs and mostly propagate eastward. The durations and maximum extents of QS MCSs show no obvious differences among different months, while those of OM MCSs vary among different months. The lowest brightness temperatures of QS MCSs mostly appear in the afternoon (0800–0900 UTC), but those of the OM MCSs exhibit no obvious diurnal variation. Compared to the OM MCSs, the QS MCSs show notable diurnal variation in intensity and develop more rapidly.
- Circulations at 0000 UTC of 285 MCS days, without direct influences from tropical cyclones, are classified into 3 patterns using the k-means algorithm. The composite circulation of P1 is consistent with the typical circulation of the Mei-yu front, and those of P2 and P3 are dominated by the northwesterly and the weak southerly, respectively. The mean initiation frequencies of the QS MCSs in P1 and P3 are the same and that in P2 is the lowest. The OM MCSs are initiated the most in P1, followed by P2, and they are initiated the least in P3.
- Analysis of the environmental conditions favorable for MCS initiation in the three circulation patterns suggests that a) the low-level wind speed in P1 is relatively high, and the MCS initiations in P1 may be accompanied by low-level jets, which is more favorable for OM MCS initiation and propagation; b) the circulation in P2 is dominated by northwesterlies with a relatively stable layer in the low-level troposphere; and c) surface solar heating in P3 establishes a dry-adiabatic or even a superadiabatic layer and further lowers the stability.



## TAKE-HOME MESSAGES

- The initiations of mesoscale convective systems are backward tracked through a hybrid method of areal overlapping and optical flow.
- Quasistationary and outward-moving mesoscale convective systems show notable differences in initiation and developments.
- A synoptic circulation pattern associated with the Mei-yu front is most favorable for the initiation of mesoscale convective systems.

# REFERENCES

- Ai, Y., Li, W., Meng, Z., & Li, J. (2016). Life Cycle Characteristics of MCSs in Middle East China Tracked by Geostationary Satellite and Precipitation Estimates. *Monthly Weather Review*, 144(7), 2517–2530. <https://doi.org/10.1175/MWR-D-15-0197.1>
- Augustine, J. A., & Howard, K. W. (1988). Mesoscale convective complexes over the United States during 1985. *Monthly Weather Review*, 116(3), 685–701. [https://doi.org/10.1175/1520-0493\(1988\)116<0685:MCCOTU>2.0.CO;2](https://doi.org/10.1175/1520-0493(1988)116<0685:MCCOTU>2.0.CO;2)
- Feng, Z., Leung, L. R., Houze, R. A., Hagos, S., Hardin, J., Yang, Q., Han, B., & Fan, J. (2018). Structure and evolution of mesoscale convective systems: sensitivity to cloud microphysics in convection-permitting simulations over the United States. *Journal of Advances in Modeling Earth Systems*, 10(7), 1470–1494. <https://doi.org/10.1029/2018MS001305>
- Feng, Z., Houze, R. A., Leung, L. R., Song, F., Hardin, J. C., Wang, J., Gustafson, W. I., & Homeyer, C. R. (2019). Spatiotemporal characteristics and large-scale environments of mesoscale convective systems east of the Rocky Mountains. *Journal of Climate*, 32(21), 7303–7328. <https://doi.org/10.1175/JCLI-D-19-0137.1>
- Hersbach, H., Bell, B., Berrisford, P., Hirahara, S., Horányi, A., Muñoz-Sabater, J., et al. (2020). The ERA5 global reanalysis. *Quarterly Journal of the Royal Meteorological Society*, 146(730), 1999–2049. <https://doi.org/10.1002/qj.3803>
- Hoffmann, P., & Schlünzen, K. H. (2013). Weather pattern classification to represent the urban heat island in present and future climate. *Journal of Applied Meteorology and Climatology*, 52(12), 2699–2714. <https://doi.org/10.1175/JAMC-D-12-065.1>
- Huth, R., Beck, C., Philipp, A., Demuzere, M., Ustrnul, Z., Cahynová, M., et al. (2008). Classifications of atmospheric circulation patterns. *Annals of the New York Academy of Sciences*, 1146(1), 105–152. <https://doi.org/10.1196/annals.1446.019>
- Lu, X., Yu, H., Ying, M., Zhao, B., Zhang, S., Lin, L., et al. (2021). Western North Pacific tropical cyclone database created by the China Meteorological Administration. *Advances in Atmospheric Sciences*, 38(4), 690–699. <https://doi.org/10.1007/s00376-020-0211-7>
- Maddox, R. A. (1980). Mesoscale convective complexes. *Bulletin of the American Meteorological Society*, 61(11), 1374–1400. [https://doi.org/10.1175/1520-0477\(1980\)061<1374:MCC>2.0.CO;2](https://doi.org/10.1175/1520-0477(1980)061<1374:MCC>2.0.CO;2)
- Roberts, R. D., & Rutledge, S. (2003). Nowcasting storm initiation and growth using GOES-8 and WSR-88D data. *Weather and Forecasting*, 18(4), 562–584. [https://doi.org/10.1175/1520-0434\(2003\)018<0562:NSIAGU>2.0.CO;2](https://doi.org/10.1175/1520-0434(2003)018<0562:NSIAGU>2.0.CO;2)
- Rousseeuw, P. J. (1987). Silhouettes: A graphical aid to the interpretation and validation of cluster analysis. *Journal of Computational and Applied Mathematics*, 20, 53–65. [https://doi.org/10.1016/0377-0427\(87\)90125-7](https://doi.org/10.1016/0377-0427(87)90125-7)
- Tang, Y., Huang, A., Wu, P., Huang, D., Xue, D., & Wu, Y. (2021). Drivers of Summer Extreme Precipitation Events Over East China. *Geophysical Research Letters*, 48(11). <https://doi.org/10.1029/2021GL093670>
- Williams, M., & Houze, R. A. (1987). Satellite-observed characteristics of winter monsoon cloud clusters. *Monthly Weather Review*, 115(2), 505–519. [https://doi.org/10.1175/1520-0493\(1987\)115<0505:SOCOWM>2.0.CO;2](https://doi.org/10.1175/1520-0493(1987)115<0505:SOCOWM>2.0.CO;2)
- Yang, J., Zhang, Z., Wei, C., Lu, F., & Guo, Q. (2017). Introducing the new generation of Chinese geostationary weather satellites, Fengyun-4. *Bulletin of the American Meteorological Society*, 98(8), 1637–1658. <https://doi.org/10.1175/BAMS-D-16-0065.1>
- Yang, R., Zhang, Y., Sun, J., & Li, J. (2020). The comparison of statistical features and synoptic circulations between the eastward-propagating and quasi-stationary MCSs during the warm season around the second-step terrain along the middle reaches of the Yangtze River. *Science China Earth Sciences*, 63(8), 1209–1222. <https://doi.org/10.1007/s11430-018-9385-3>
- Ying, M., Zhang, W., Yu, H., Lu, X., Feng, J., Fan, Y., et al. (2014). An overview of the China Meteorological Administration tropical cyclone database. *Journal of Atmospheric and Oceanic Technology*, 31(2), 287–301. <https://doi.org/10.1175/JTECH-D-12-00119.1>
- Zhang, F., Zhang, Q., & Sun, J. (2021). Initiation of an Elevated Mesoscale Convective System With the Influence of Complex Terrain During Meiyu Season. *Journal of Geophysical Research: Atmospheres*, 126(1), e2020JD033416. <https://doi.org/10.1029/2020JD033416>
- Zhang, X., Shen, W., Zhuge, X., Yang, S., Chen, Y., Wang, Y., et al. (2021). Statistical Characteristics of Mesoscale Convective Systems Initiated over the Tibetan Plateau in Summer by Fengyun Satellite and Precipitation Estimates. *Remote Sensing*, 13(9). <https://doi.org/10.3390/rs13091652>



# TANK YOU !



[sjh@mail.iap.ac.cn](mailto:sjh@mail.iap.ac.cn)

[fuyanan20@mails.ucas.ac.cn](mailto:fuyanan20@mails.ucas.ac.cn)

